

Metastability and dynamic modes in magnetic island chains

G. M. Wysin*

Department of Physics, Kansas State University, Manhattan, KS 66506-2601

(Dated: October 24, 2021)

The uniform states of a model for one-dimensional chains of thin magnetic islands on a nonmagnetic substrate coupled via dipolar interactions are described here. Magnetic islands oriented with their long axes perpendicular to the chain direction are assumed, whose shape anisotropy imposes a preference for the dipoles to point perpendicular to the chain. The competition between anisotropy and dipolar interactions leads to three types of uniform states of distinctly different symmetries, including metastable transverse or remanent states, transverse antiferromagnetic states, and longitudinal states where all dipoles align with the chain direction. The stability limits and normal modes of oscillation are found for all three types of states, even including infinite range dipole interactions. The normal mode frequencies are shown to be determined from the eigenvalues of the stability problem.

Keywords: magnetics, magnetic islands, frustration, dipole interactions, metastability, magnon modes.

I. ARRAYS OF MAGNETIC ISLANDS

Artificial spin lattices can be fabricated from thin elongated magnetic islands arranged on a nonmagnetic substrate, such as in one-dimensional (1D) artificial spin chains [1–3] and two-dimensional (2D) artificial spin ice systems[4]. The competition of strong shape anisotropy with dipolar interactions in artificial spin ice with two-state Ising-like [5, 6] dipoles leads to a ground state that follows an ice rule [7–9], with antiferromagnetic order in square artificial spin ice. There are also metastable excited remanent states of nonzero average magnetic moment, that result from the application of an applied magnetic field which is slowly turned off. The different low energy ground and remanent states possess distinctive modes of oscillation relative to those states [10–13], that can serve as signatures [14, 15] of those states.

In particular for 1D artificial spin systems, Östman *et al.* [2] fabricated and analyzed chains of mesoscopic magnetic islands with strong shape anisotropy (due to a high aspect ratio), which causes the effective spins to behave as Ising-like. Nguyen *et al.* [1] considered how slight changes from 1D to quasi-2D lattice structure can affect the lowest states of artificial Ising spins, especially due to the geometric dependence of the dipole interactions. Cisternas *et al.* [3] considered a model for a chain of a few coupled XY magnetic dipoles with rotational inertia (magnetic charges on dumbbells with one angular coordinate) and the stability of its dynamic solutions. Alternatively, we consider a model for a chain of artificial spins with easy-plane shape anisotropy and weak uniaxial shape anisotropy within the easy plane, such that their behavior is not Ising-like, but rather, more closely described by three-component Heisenberg-like [16, 17] dipoles. This model applies to a set of thin and some-

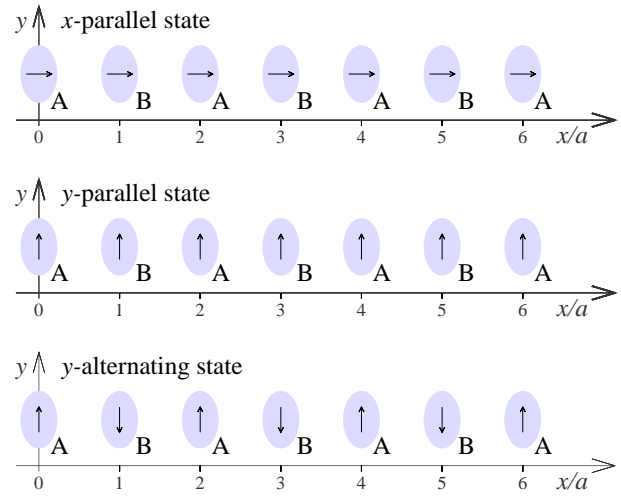


FIG. 1: The three uniform states of a chain of elongated magnetic islands separated by lattice constant a , with long axes perpendicular to the chain direction.

what elongated magnetic islands fabricated on a nonmagnetic substrate. The possible stable and metastable uniform states are analyzed for varying uniaxial anisotropy strength K_1 of the individual islands, relative to the effective strength of nearest neighbor dipole interactions, D . For fixed island shapes and center-to-center separations a , the energy constants K_1 , D and an easy-plane anisotropy strength K_3 are determined by the thickness and aspect ratio of the islands [18]. However, K_1 and D might be modified post-fabrication by pressure or elastic strain [19], or other yet to be found methods.

The chain is taken along the x -direction, with elongated magnetic islands whose long axes are arranged perpendicular (along y) to the chain, see Fig. 1. This is inspired by the geometry of a row of islands in artificial square lattice spin ice, however, the physics is different due to the one-dimensionality and the geometrical dependence of the dipolar interactions. The most interesting

*Electronic address: wysin@phys.ksu.edu;
URL: <http://www.phys.ksu.edu/personal/wysin>

effects take place for relatively weak uniaxial anisotropy K_1 relative to D , that would correspond to slightly elongated islands, as shape anisotropy is the result of unequal demagnetization effects along the short and long axes of the islands. The Heisenberg-like island dipoles are assumed to be of fixed magnitude and able to point in any direction, but have energetic *preferences* for staying in the plane of the substrate, and for aligning with the islands' long axes.

With long axes perpendicular to the chain, the islands' dipole moments will tend to point perpendicular to the chain direction to minimize the shape anisotropy energy. Then nearest neighbor dipolar interactions will impose a transverse alternating or antiferromagnetic (AFM) state (neighboring dipoles along $\pm\hat{y}$) for simultaneously minimizing the dipolar energy. This AFM y -alternating state, depicted in Fig. 1, is reminiscent of a row in a ground state of square lattice artificial spin ice.

Other possible uniform states are depicted in Fig. 1. If a uniform magnetic field is applied perpendicular to the chain, and then turned off, it can leave the system in a corresponding metastable remanent or y -parallel state, where the dipoles either all point along $+\hat{y}$ or all along $-\hat{y}$, with ferromagnetic order transverse to the chain. A uniform magnetic field applied parallel to the chain, and then turned off, could leave all the dipoles uniformly aligned with the chain direction, in an x -parallel state, with ferromagnetic order longitudinally along the chain, but only if dipolar interactions dominate over the shape anisotropy (D larger than K_1). Nonuniform excited states, such as single dipole reversals from any of the uniform states, are not considered here.

The calculations here determine the static structure, the conditions for stability, and the linearized normal modes of oscillation for all three uniform states. The stability analysis gives eigenvalues that are shown to connect directly to the dynamic mode frequencies. The description here is initially developed for a nearest neighbor model, and then extended to include infinite range dipolar interactions for an infinite chain. The analysis is based on classical undamped spin dynamics, treating each island as a single macro-magnetic moment in the macrospin approximation used previously by Wysin *et al.*[20, 21] and by Iacocca *et al.*[10]. While the macrospin assumption is certainly an approximation for a real-life magnetic island structure, the calculations should give some reasonable representation of what could happen in this type of engineered magnetic array, especially for adequately spaced islands where the neighbors' dipolar fields are quasi-uniform within an island [22].

II. THE MAGNETIC ISLAND MODEL

The dipoles are initially assumed to interact via nearest neighbor dipole interactions, together with uniaxial anisotropy (along \hat{y} , parameter $K_1 > 0$) perpendicular to the chain and easy-plane anisotropy (xy -plane, parame-

ter $K_3 > 0$) as expected for thin islands of soft magnetic material on a substrate. The 1D chain has N dipoles $\mu\mathbf{S}_n$, where \mathbf{S}_n are three-component dimensionless unit spin vectors separated by lattice constant a . The nearest neighbor dipolar interaction constant is

$$D = \frac{\mu_0\mu^2}{4\pi a^3}. \quad (1)$$

The Hamiltonian for the chain is

$$H = \sum_{n=1}^N \{D[\mathbf{S}_n \cdot \mathbf{S}_{n+1} - 3(\mathbf{S}_n \cdot \hat{x})(\mathbf{S}_{n+1} \cdot \hat{x})] - K_1 (S_n^y)^2 + K_3 (S_n^z)^2\}. \quad (2)$$

The dipolar interactions make neighboring dipole prefer to be perpendicular to the chain direction and antiparallel to each other. The system can be analyzed as a two-sublattice problem. This is most relevant for the y -alternating states. Therefore, we introduce A and B sublattices, for the odd and even sites, respectively. Let the spins now be labelled as $\mathbf{S}_n \rightarrow \mathbf{A}_n$, and $\mathbf{S}_{n+1} \rightarrow \mathbf{B}_{n+1}$, for $n = 1, 3, 5, \dots, N$. A two-spin cell becomes the basic unit in the Hamiltonian.

A. The uniform low energy states

Initially, the static low-energy states are to be found. Those have uniform aligned spins on each sublattice. Let sublattice spin vectors \mathbf{A} and \mathbf{B} define the state. A pair of neighboring sites has two bonds and anisotropy terms for both sites. The two-site Hamiltonian H_{AB} is twice the energy per site u :

$$H_{AB} = 2u = 2D [\mathbf{A} \cdot \mathbf{B} - 3(\mathbf{A} \cdot \hat{x})(\mathbf{B} \cdot \hat{x}) - K_1 (A_y^2 + B_y^2) + K_3 (A_z^2 + B_z^2)]. \quad (3)$$

It is convenient to express the spins using out-of-plane and azimuthal angles (θ, ϕ) as in $\mathbf{S} = (\cos\theta \cos\phi, \cos\theta \sin\phi, \sin\theta)$, which gives

$$H_{AB} = 2D [\sin\theta_A \sin\theta_B + \cos\theta_A \cos\theta_B (-2 \cos\phi_A \cos\phi_B + \sin\phi_A \sin\phi_B)] - K_1 (\cos^2\theta_A \sin^2\phi_A + \cos^2\theta_B \sin^2\phi_B) + K_3 (\sin^2\theta_A + \sin^2\theta_B) \quad (4)$$

Minimization of H_{AB} with respect to the four angles leads to the possible states. The islands are thin along the z -direction, which causes strong easy-plane (K_3) anisotropy so that static solutions are planar, having $\theta_A = \theta_B = 0$. Deviations of θ_A and θ_B away from zero are assumed in the stability analysis (Sec. II B) and are present in the dynamic solutions (Sec. III). There remains,

$$\frac{\partial H_{AB}}{\partial \phi_A} = 2 \{D(2 \sin\phi_A \cos\phi_B + \cos\phi_A \sin\phi_B) - K_1 \sin\phi_A \cos\phi_A\} = 0, \quad (5)$$

together with the same relation with A and B interchanged. These equations have three physically distinct uniform-state solutions: (1) x -parallel states, with $\phi_A = \phi_B = 0$ or $\phi_A = \phi_B = \pi$; (2) y -parallel states, with $\phi_A = \phi_B = \pm\frac{\pi}{2}$; and (3) y -alternating states, with $\phi_A = -\phi_B = \pm\frac{\pi}{2}$. All are doubly degenerate. The x -parallel states have large anisotropy energy, while reducing their dipolar energy, while the y -alternating states tend to have low anisotropy energy and low dipolar energy. The y -parallel states are intermediate; their anisotropy energy is low but their dipolar energy is high.

An indication of the stabilities of these states is obtained from the resulting energies per AB pair. Consider planar states with $\theta_A = \theta_B = 0$. For aligned sublattices ($\phi_A = \phi_B$), the two-site energy $H_{AB}(\phi_A, \phi_B)$ becomes

$$H_{AB}(\phi_A, \phi_A) = -4D + 2(3D - K_1) \sin^2 \phi_A. \quad (6)$$

This suggests that an x -parallel state (say, $\phi_A = \phi_B = 0$) will be destabilized when $K_1 > 3D$, because any small deviation in ϕ_A will lower the energy. At the same time, it suggests that a y -parallel state (say, $\phi_A = \phi_B = \frac{\pi}{2}$) will be destabilized when $K_1 < 3D$. A similar analysis can be applied to states with antialigned sublattices ($\phi_A = -\phi_B$), where the two-site energy is

$$H_{AB}(\phi_A, -\phi_A) = -4D + 2(D - K_1) \sin^2 \phi_A. \quad (7)$$

Considering small deviations around $\phi_A = 0$, this shows the x -parallel states to be stable for $K_1 < D$, but unstable for $K_1 > D$. Considering instead deviations around a state with $\phi_A = \frac{\pi}{2}$ indicates that the y -alternating states will be unstable for $K_1 < D$ but stable for $K_1 > D$. The per-site energies $u(\phi_A, \phi_B) = \frac{1}{2}H_{AB}$ and stability requirements are summarized as follows:

$$\begin{aligned} x\text{-parallel: } u(0, 0) &= -2D, & K_1 < D, \\ y\text{-parallel: } u\left(\frac{\pi}{2}, \frac{\pi}{2}\right) &= -K_1 + D, & K_1 > 3D, \\ y\text{-alternating: } u\left(\frac{\pi}{2}, -\frac{\pi}{2}\right) &= -K_1 - D, & K_1 > D. \end{aligned} \quad (8)$$

These estimates from the nearest neighbor model are plotted as functions of K_1 for fixed D in Fig. 2. The y -parallel states become lower than x -parallel when they appear at $K_1 > 3D$, and the y -alternating states are lower than both x -parallel and y -parallel when they appear at $K_1 > D$. The y -parallel states apparently are metastable, falling between the other two states for $K_1 > 3D$. Starting from an alternating state, the system might arrive at a y -parallel state through the application of an external magnetic field along y , which is then removed, making it a remanent-like state. Such a state is expected to be locally stable against *small* perturbations even though lower energy states exist below it.

B. Planar state energetic stability?

The states found above must have a requirement on the easy-plane anisotropy (K_3) needed to maintain local energetic stability (against weak perturbations). It is

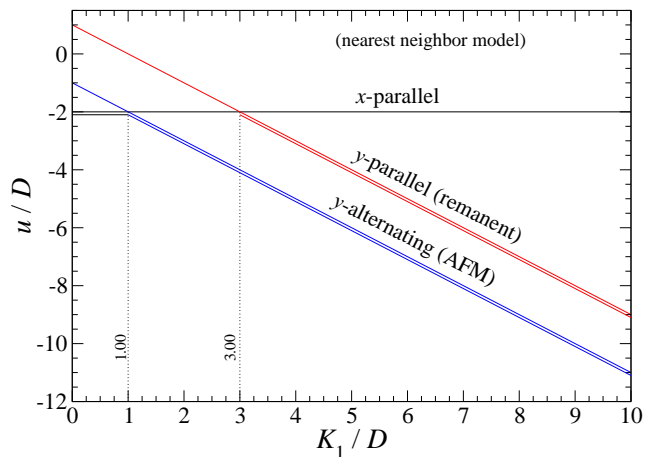


FIG. 2: The static per-site energy densities u of the three planar metastable states, versus scaled uniaxial anisotropy. The x -parallel state is stable only for $K_1 < D$, y -alternating only for $K_1 > D$, and y -parallel only for $K_1 > 3D$. Double (single) lines indicate local stability (instability) against weak perturbations. Dynamic stability is shown to require $K_3 > -D$ for all three states.

important to consider small in-plane (ϕ_A, ϕ_B) and out-of-plane (θ_A, θ_B) deviations of the dipoles around each state to get a view of their local energetic stability. Let the in-plane angles become $\phi_A \rightarrow \bar{\phi}_A + \phi_A$ and $\phi_B \rightarrow \bar{\phi}_B + \phi_B$, and the out-of-plane are θ_A, θ_B , where the overbar indicates the original state, and the other angles are the deviations. In linear stability analysis, H_{AB} is expanded to quadratic order in the deviations. The energies of in-plane and out-of-plane deviations separate, with

$$H_{AB} = \bar{H} + H_\phi + H_\theta, \quad (9)$$

where \bar{H} is the unperturbed state energy and H_ϕ and H_θ are the deviation energies.

1. Stability of x -parallel states

In the x -parallel state with $\bar{\phi}_A = \bar{\phi}_B = 0$ and $\bar{H} = -4D$, the two-site deviation energies are

$$\begin{aligned} H_\phi &= (2D - K_1) (\phi_A^2 + \phi_B^2) + 2D\phi_A\phi_B, \\ H_\theta &= (2D + K_3) (\theta_A^2 + \theta_B^2) + 2D\theta_A\theta_B. \end{aligned} \quad (10)$$

These can be placed into matrix form, defining deviation vectors,

$$\psi_\theta \equiv \begin{pmatrix} \theta_A \\ \theta_B \end{pmatrix}, \quad \psi_\phi \equiv \begin{pmatrix} \phi_A \\ \phi_B \end{pmatrix}. \quad (11)$$

Then the deviation energies can be written as $H_\phi = \psi_\phi^\dagger M_\phi \psi_\phi$ and $H_\theta = \psi_\theta^\dagger M_\theta \psi_\theta$, where there is a symmetric matrix for each part. The out-of-plane matrix is

$$M_\theta = \begin{pmatrix} M_{\theta,0} & M_{\theta,1} \\ M_{\theta,1} & M_{\theta,0} \end{pmatrix} = \begin{pmatrix} 2D + K_3 & D \\ D & 2D + K_3 \end{pmatrix} \quad (12)$$

Any instability of the x -parallel state will be exhibited as excitation of an eigenvector of M_θ with a negative energy eigenvalue. Considering the eigenvalue problem written as $M_\theta\psi_\theta = \sigma_\theta\psi_\theta$, the eigenvalues σ_θ are obtained by

$$(M_{\theta,0} - \sigma_\theta)^2 - M_{\theta,1}^2 = 0 \implies \sigma_\theta^\pm = M_{\theta,0} \pm M_{\theta,1}. \quad (13)$$

There are symmetric and antisymmetric eigenvectors and their eigenvalues,

$$\psi_\theta^\pm = \frac{1}{\sqrt{2}}(1, \pm 1), \quad \sigma_\theta^+ = 3D + K_3, \quad \sigma_\theta^- = D + K_3. \quad (14)$$

Both eigenvalues are real and positive, provided $K_3 > -D$. If a deviation state is expressed as a linear combination, $\psi_\theta = c_\theta^+\psi_\theta^+ + c_\theta^-\psi_\theta^-$, then the energy can only go upwards if any such deviation occurs:

$$H_\theta = |c_\theta^+|^2 \sigma_\theta^+ + |c_\theta^-|^2 \sigma_\theta^-. \quad (15)$$

The x -parallel state is absolutely stable with respect to out-of-plane fluctuations for any $K_3 > -D$. Even when $K_3 = 0$, dipolar interactions alone provide a sufficient easy-plane anisotropy to guarantee planar stability

For in-plane deviations, the matrix is

$$M_\phi = \begin{pmatrix} M_{\phi,0} & M_{\phi,1} \\ M_{\phi,1} & M_{\phi,0} \end{pmatrix} = \begin{pmatrix} 2D - K_1 & D \\ D & 2D - K_1 \end{pmatrix}. \quad (16)$$

As the matrix has the same symmetric form as M_θ , it has the same symmetric and antisymmetric eigenvectors, but with different eigenvalues,

$$\psi_\phi^\pm = \frac{1}{\sqrt{2}}(1, \pm 1), \quad \sigma_\phi^+ = 3D - K_1, \quad \sigma_\phi^- = D - K_1. \quad (17)$$

Both eigenvalues remain positive as long as $K_1 < D$, which confirms the stability requirement for in-plane deviations found earlier for the x -parallel state. The in-plane instability for $K_1 > D$ is antisymmetric, with out-of-phase sublattice deviations ($\phi_A = -\phi_B$).

2. Stability of y -parallel (remanent) states

For the y -parallel states ($\bar{\phi}_A = \bar{\phi}_B = \pm \frac{\pi}{2}$) with unperturbed energy $\bar{H} = 2(D - K_1)$, the deviation energies $H_\theta = \psi_\theta^\dagger M_\theta \psi_\theta$ and $H_\phi = \psi_\phi^\dagger M_\phi \psi_\phi$ are determined again by symmetric matrices of the same form as encountered for x -parallel states, see Eqs. (12) and (16), but now the diagonal and off-diagonal elements for the out-of-plane deviations are

$$M_{\theta,0} = -D + K_1 + K_3, \quad M_{\theta,1} = D. \quad (18)$$

The associated eigenvalues $\sigma_\theta^\pm = M_{\theta,0} \pm M_{\theta,1}$ are

$$\sigma_\theta^+ = K_1 + K_3, \quad \sigma_\theta^- = -2D + K_1 + K_3. \quad (19)$$

Both eigenvalues stay positive and maintain stability if

$$K_1 + K_3 > 2D. \quad (20)$$

For in-plane deviations, the matrix elements are

$$M_{\phi,0} = -D + K_1, \quad M_{\phi,1} = -2D. \quad (21)$$

The eigenvalues for symmetric or antisymmetric eigenvectors are

$$\sigma_\phi^+ = -3D + K_1, \quad \sigma_\phi^- = D + K_1. \quad (22)$$

σ_ϕ^- is always positive as long as K_1 is positive, but σ_ϕ^+ will only stay positive and insure stability if $K_1 > 3D$. This is more restrictive than the out-of-plane energy eigenvalues. Then y -parallel states are energetically stable only for $K_1 > 3D$ and any $K_3 > -D$, although they are local minima or meta-stable states.

3. Stability of y -alternating (AFM-ordered) states

For the y -alternating state with $\bar{\phi}_A = \frac{\pi}{2}$ and $\bar{\phi}_B = -\frac{\pi}{2}$ and unperturbed energy $\bar{H} = -2(D + K_1)$, the same form of matrices again applies to the deviation energies. The diagonal and off-diagonal matrix elements for out-of-plane deviations are

$$M_{\theta,0} = D + K_1 + K_3, \quad M_{\theta,1} = D, \quad (23)$$

which gives the eigenvalues,

$$\sigma_\theta^+ = 2D + K_1 + K_3, \quad \sigma_\theta^- = K_1 + K_3. \quad (24)$$

These are always positive so there is no instability with respect to out-of-plane motions. For in-plane deviations, the corresponding matrix elements are

$$M_{\phi,0} = D + K_1, \quad M_{\phi,1} = 2D, \quad (25)$$

which gives the eigenvalues that determine stability,

$$\sigma_\phi^+ = 3D + K_1, \quad \sigma_\phi^- = -D + K_1. \quad (26)$$

Here σ_ϕ^+ is always positive, but $\sigma_\phi^- > 0$ requires $K_1 > D$ for stability against in-plane fluctuations. One also sees $K_3 > -D$ is the limiting condition for planar stability.

Therefore this energetic stability analysis confirms and expands upon the results of Eq. (8). At $K_1 < D$, x -parallel states are the only stable ones. With increasing K_1 , the y -alternating states become stable at $K_1 > D$, exactly at the point where the x -parallel states become destabilized. Even more interesting is that the y -parallel states become stable only for $K_1 > 3D$, when their energy falls *below* the already unstable x -parallel states, but *above* the y -alternating states, see Fig. 2, where local stability (instability) is indicated by double (single) lines. For $K_1 > 3D$, both y -parallel and y -alternating states are linearly stable against small perturbations. For planar stability, $K_3 > -D$ is required for all three uniform states. Thus the original assumption of easy-plane anisotropy ($K_3 > 0$) can be relaxed, as the dipolar interactions themselves produce a weak easy-plane anisotropy.

III. NORMAL MODE OSCILLATIONS AROUND THE STATES

Now the linearized dynamics of the full chain is solved (beyond the two-site Hamiltonian). It is shown that the dynamic oscillation mode frequencies are directly connected to the energy eigenvalues above. Any site has two nearest neighbors that exert torques on it (in the nearest neighbor approximation). The magnetic dipole vectors are $\vec{\mu}_n = \mu \mathbf{S}_n$, of magnitude μ with dimensionless spin vectors \mathbf{S}_n , and supposing a gyromagnetic ratio γ , they follow undamped dynamics from Hamiltonian (2), using dot to indicate time derivative [23],

$$\frac{1}{\gamma} \dot{\vec{\mu}}_n = \vec{\mu}_n \times \left(-\frac{\partial H}{\partial \vec{\mu}_n} \right). \quad (27)$$

A simplified way to write this is

$$\dot{\mathbf{S}}_n = \mathbf{S}_n \times \mathbf{F}_n, \quad (28)$$

where the Hamiltonian becomes $H = -\sum_n \mathbf{S}_n \cdot \mathbf{F}_n$ and the effective magnetic field on a site is $\mathbf{F}_n = -\partial H / \partial \mathbf{S}_n$,

$$\mathbf{F}_n = \kappa_1 S_n^y \hat{y} - \kappa_3 S_n^z \hat{z} + \delta_1 \sum_{k=n\pm 1} [3(\mathbf{S}_k \cdot \hat{x}) \hat{x} - \mathbf{S}_k]. \quad (29)$$

The coupling parameters are

$$\kappa_1 \equiv \frac{2\gamma K_1}{\mu}, \quad \kappa_3 \equiv \frac{2\gamma K_3}{\mu}, \quad \delta_1 \equiv \frac{\gamma D}{\mu}. \quad (30)$$

The effective field components are

$$\begin{aligned} F_n^x &= 2\delta_1 (S_{n-1}^x + S_{n+1}^x), \\ F_n^y &= -\delta_1 (S_{n-1}^y + S_{n+1}^y) + \kappa_1 S_n^y, \\ F_n^z &= -\delta_1 (S_{n-1}^z + S_{n+1}^z) - \kappa_3 S_n^z. \end{aligned} \quad (31)$$

The oscillations take place relative to one of the three metastable states, whose unperturbed spin components are $\bar{\mathbf{S}}_n = (\bar{S}_n^x, \bar{S}_n^y, 0)$, so that

$$\mathbf{S}_n = (\bar{S}_n^x + s_n^x, \bar{S}_n^y + s_n^y, s_n^z), \quad (32)$$

where $\mathbf{s}_n(t) = (s_n^x, s_n^y, s_n^z)$ are the small-amplitude time-dependent deviations. These can also be expressed in terms of in-plane and out-of-plane angular deviations. The equations of motion (28) are linearized in $\mathbf{s}_n(t)$, which leads to wave equations for the normal modes for each type of metastable state.

A. Dynamics in the x -parallel states

In an x -parallel state, $\bar{S}_n^x = 1$ and $\bar{S}_n^y = 0$ hold uniformly at all sites. After linearization, the equations of motion imply $s_n^x = 0$ and fixed spin length. The in-plane and out-of-plane components satisfy

$$\begin{aligned} \dot{s}_n^y &= +\delta_1 (4s_n^z + s_{n-1}^z + s_{n+1}^z) + \kappa_3 s_n^z, \\ \dot{s}_n^z &= -\delta_1 (4s_n^y + s_{n-1}^y + s_{n+1}^y) + \kappa_1 s_n^y. \end{aligned} \quad (33)$$

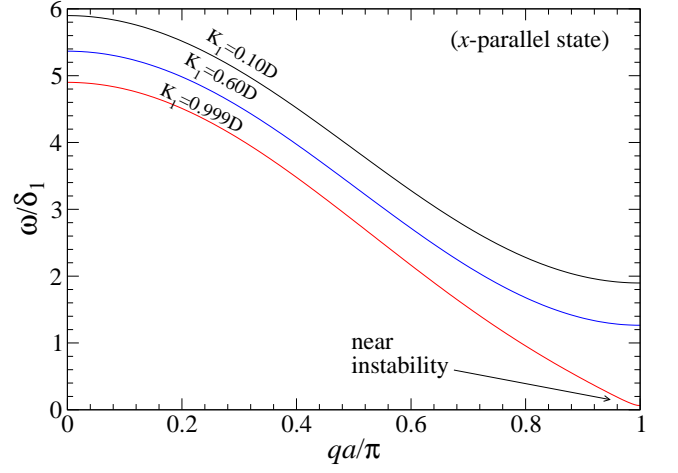


FIG. 3: The mode frequencies for a x -parallel state in the nearest neighbor model, with $K_3 = 0$, and indicated values of $K_1 < D$. The modes produce instability ($\omega \rightarrow 0$) at $qa = \pi$ as $K_1 \rightarrow D$.

These are solved by traveling waves of the form $s_n^y(t) = s^y \exp[i(qna - \omega t)]$ and similar for the z -component, where s^y is an amplitude, q is the wave vector, and ω is the frequency. The resulting dispersion relation is

$$\frac{\omega}{4\delta_1} = \sqrt{\left(1 + \frac{1}{2} \cos qa - \frac{K_1}{2D}\right) \left(1 + \frac{1}{2} \cos qa + \frac{K_3}{2D}\right)}. \quad (34)$$

Examples are plotted in Fig. 3, showing the maximum frequency at $q = 0$, and a gap at $qa = \pi$ that depends on the anisotropy. That gap goes to zero when instability occurs. At the limit $qa = \pi$, both factors in the square root in (34) remain positive and imply real frequencies (and stability) of x -parallel states as long as

$$K_1 < D \quad \text{and} \quad K_3 > -D. \quad (35)$$

To the contrary, an imaginary frequency signals instability if $K_1 > D$ or $K_3 < -D$. The latter condition means that even when $K_3 = 0$ as used in Fig. 3 (i.e., no easy-plane anisotropy), the dipolar interactions work to stabilize a planar state of the dipoles. This holds for all three uniform states, see below.

These conditions on the anisotropy parameters verify the earlier energetic stability analysis of x -parallel states. In addition, the point where instability first appears corresponds to $qa = \pi$ for $K_1 = D$, with an excitation that is out-of-phase on neighboring sites. It agrees with the finding that the energy eigenvalue $\sigma_\phi^- = D - K_1$ associated with the antisymmetric eigenvector ψ_ϕ^- becomes negative for $K_1 > D$, see Eq. (14).

B. Dynamics in the y -parallel states

In a y -parallel state, $\bar{S}_n^x = 0$ and $\bar{S}_n^y = 1$ hold uniformly at all sites. Now the deviation s_n^y is zero when

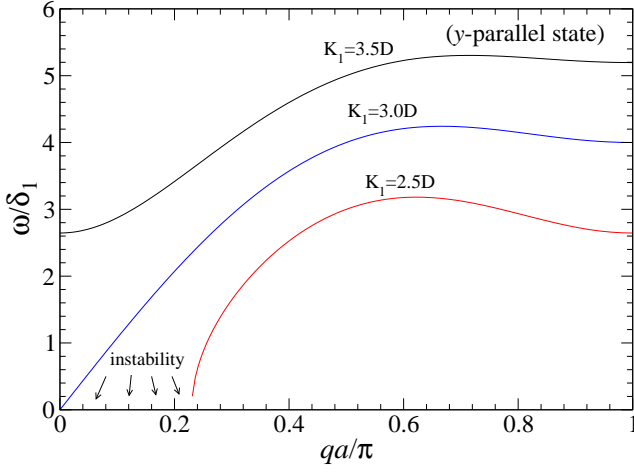


FIG. 4: The mode frequencies for a y -parallel state in the nearest neighbor model with $K_3 = 0$, and indicated uniaxial anisotropies K_1 . The states require $K_1 > 3D$ for real frequencies and stability. The modes produce instability with $K_1 < 3D$, leading to imaginary ω near $qa = 0$.

the equations are linearized, and there remains oscillating in-plane and out-of-plane time-dependent deviations that follow

$$\begin{aligned} \dot{s}_n^x &= +\delta_1 (2s_n^z - s_{n-1}^z - s_{n+1}^z) - \kappa_{13}s_n^z, \\ \dot{s}_n^z &= -2\delta_1 (s_n^x + s_{n-1}^x + s_{n+1}^x) + \kappa_{13}s_n^x, \end{aligned} \quad (36)$$

where the combined anisotropy constant is $\kappa_{13} \equiv \kappa_1 + \kappa_3$. Traveling waves solve this system. Defining $K_{13} \equiv K_1 + K_3$, the dispersion relation is

$$\frac{\omega}{2\delta_1} = \sqrt{(1 + 2\cos qa - \frac{K_1}{D})(1 - \cos qa - \frac{K_{13}}{D})}. \quad (37)$$

The typical behavior of $\omega(q)$ is plotted in Fig. 4 for $K_3 = 0$ and various values of K_1 . The frequency must remain real for stability. This requires both factors inside the square root to be negative, such that their product is positive. That leads to the conditions for stability of y -parallel states,

$$K_1 + K_3 > 2D \quad \text{and} \quad K_1 > 3D. \quad (38)$$

These imply the separated stability requirements,

$$K_1 > 3D \quad \text{and} \quad K_3 > -D. \quad (39)$$

The dipolar interactions by themselves already insure planar stability and easy-plane anisotropy is not essential.

The value of $K_1 - 3D$ controls the size of the gap at $q = 0$. On the other hand, once $K_1 < 3D$ the uniaxial anisotropy is too weak to stabilize the y -parallel states. This is the same stability limit as found in the energy eigenvalue analysis. Also, the instability takes place now at $qa = 0$, where the second factor in the square root of the dispersion relation changes from negative to positive

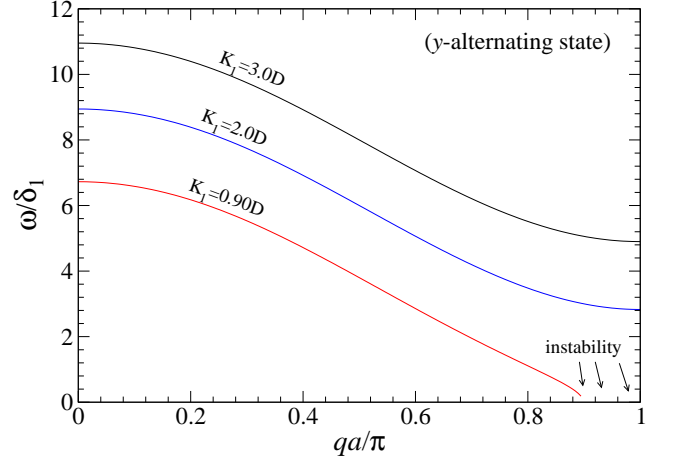


FIG. 5: The mode frequencies for a y -alternating state in the nearest neighbor model, with $K_3 = 0$, and $K_1 > D$ needed for real frequencies and stability. The modes produce instability (imaginary ω) for example with $K_1 = 0.90D$ near $qa = \pi$.

for $K_1 < 3D$. This is reflected in the energy eigenvalue $\sigma_\phi^+ = -3D + K_1$ becoming negative for $K_1 < 3D$, and leading to in-phase in-plane deviations of the dipoles (i.e., ψ_ϕ^+) as the excitation driving the instability. Once y -parallel becomes unstable, the configuration should tend towards one of the stable y -alternating states.

C. Dynamics in the y -alternating states

Finally consider the y -alternating state with $\bar{S}_n^x = \bar{S}_{n+1}^x = 0$ and $\bar{S}_n^y = +1$, $\bar{S}_{n+1}^y = -1$, for $n = 1, 3, 5, \dots$. It is better to denote the spin deviations by sublattices, and let $s_n^x \rightarrow a_n^x$ and $s_n^z \rightarrow a_n^z$ on the A-sublattice (odd sites n) and $s_{n+1}^x \rightarrow b_{n+1}^x$ with $s_{n+1}^z \rightarrow b_{n+1}^z$ on the B-sublattice (even sites $n + 1$). Any deviations in y -components are zero when the system is linearized. The dynamic equations on the A-sites are

$$\begin{aligned} \dot{a}_n^x &= -\delta_1 (2a_n^z + b_{n-1}^z + b_{n+1}^z) - \kappa_{13}a_n^z, \\ \dot{a}_n^z &= +2\delta_1 (a_n^x - b_{n-1}^x - b_{n+1}^x) + \kappa_{13}a_n^x. \end{aligned} \quad (40)$$

With the B-sites in an opposite unperturbed direction, their time derivative equations have reversed signs,

$$\begin{aligned} \dot{b}_n^x &= +\delta_1 (2b_n^z + a_{n-1}^z + a_{n+1}^z) + \kappa_{13}b_n^z, \\ \dot{b}_n^z &= -2\delta_1 (b_n^x - a_{n-1}^x - a_{n+1}^x) - \kappa_{13}b_n^x. \end{aligned} \quad (41)$$

These equations are solved by traveling waves such as $a_n^x(t) = a^x \exp[i(qna - \omega t)]$ and similar for the other components, however, it is necessary to form linear combinations of the fields on the two sublattices.

Consider the linear combination that is antisymmetric in-plane but symmetric out-of-plane, defined by

$$\mathbf{g}_n = (g_n^x, g_n^z) \equiv (a_n^x - b_n^x, a_n^z + b_n^z). \quad (42)$$

This produces a system in only this one field,

$$\begin{aligned}\dot{g}_n^x &= -\delta_1 (2g_n^z + g_{n-1}^z + g_{n+1}^z) - \kappa_{13}g_n^z, \\ \dot{g}_n^z &= +2\delta_1 (g_n^x + g_{n-1}^x + g_{n+1}^x) + \kappa_1g_n^x.\end{aligned}\quad (43)$$

The resulting dispersion relation for the ‘‘g-modes’’ is

$$\frac{\omega_g}{2\delta_1} = \sqrt{(1 + 2\cos qa + \frac{K_1}{D})(1 + \cos qa + \frac{K_{13}}{D})}. \quad (44)$$

This is plotted in Fig. 5 for $K_3 = 0$ and various values of K_1 . Now the frequency remains real provided both factors inside the square root remain positive. At the value $\cos qa = -1$, this leads to the conditions for stability,

$$K_1 + K_3 > 0 \quad \text{and} \quad K_1 > D. \quad (45)$$

These imply $K_3 > -D$; dipolar interactions by themselves can provide planar stability. The condition $K_1 > D$ holds as long as the in-plane energy eigenvalue $\sigma_\phi^- = -D + K_1$ remains positive. Otherwise, when $K_1 < D$, the modes of y -alternating states will be destabilized by an excitation at $qa = \pi$. Due to the construction of the g -field, that excitation will contain in-plane components that are in-phase on the two sublattices, while the out-of-plane components will be out-of-phase. The destabilization will tend to drive the system into one of the (stable) x -parallel states. The size of the nonzero gap at $qa = \pi$ is determined by $K_1 - D$.

Another linear combination that is symmetric in-plane but antisymmetric out-of-plane can be defined by

$$\mathbf{h}_n = (h_n^x, h_n^z) \equiv (a_n^x + b_n^x, a_n^z - b_n^z). \quad (46)$$

This dynamics of this field is

$$\begin{aligned}\dot{h}_n^x &= -\delta_1 (2h_n^z + h_{n-1}^z + h_{n+1}^z) - \kappa_{13}h_n^z, \\ \dot{h}_n^z &= +2\delta_1 (h_n^x - h_{n-1}^x - h_{n+1}^x) + \kappa_1h_n^x.\end{aligned}\quad (47)$$

The ‘‘h-modes’’ here have the dispersion relation

$$\frac{\omega_h}{2\delta_1} = \sqrt{(1 - \cos qa + \frac{K_{13}}{D})(1 - 2\cos qa + \frac{K_1}{D})}. \quad (48)$$

One can see that $\omega_h(q) = \omega_g(q + \frac{\pi}{a})$. Therefore this set of solutions is already contained in the g -modes, and leads to the same condition, $K_1 > D$, for stability of the y -alternating states.

IV. CONNECTING THE DYNAMIC FREQUENCIES TO THE ENERGY EIGENVALUES

In classical mechanics, an out-of-plane spin component $S^z = \sin\theta$ is the momentum conjugate to the in-plane spin angle ϕ for a site. In the two-sublattice model, the Hamilton equations of motion are obtained from the energy H_{AB} by

$$\frac{\mu}{\gamma} \frac{d}{dt} \phi = \frac{\partial H_{AB}}{\partial \sin\theta}, \quad \frac{\mu}{\gamma} \frac{d}{dt} \sin\theta = -\frac{\partial H_{AB}}{\partial \phi}. \quad (49)$$

The energy $H_{AB} = 2u$ assumes two uniform sublattices, and gives dynamics of a central A or central B site, with two AB bonds contributing to the energy. The Hamiltonian is like that for a set of coupled oscillators, where squared θ 's are kinetic energies and squared ϕ 's are spring energies. Considering small amplitude oscillations, $\sin\theta$ can be replaced by θ for each sublattice. Using states $\psi_\phi^\dagger \equiv (\phi_A, \phi_B)$ and $\psi_\theta^\dagger \equiv (\theta_A, \theta_B)$, the linearized matrix expressions for $H_{AB} = 2u$ are of quadratic form,

$$\begin{aligned}H_{AB} &\approx \bar{H} + \psi_\phi^\dagger M_\phi \psi_\phi + \psi_\theta^\dagger M_\theta \psi_\theta \\ &= \bar{H} + M_{\phi,0} (\phi_A^2 + \phi_B^2) + 2M_{\phi,1} \phi_A \phi_B \\ &\quad + M_{\theta,0} (\theta_A^2 + \theta_B^2) + 2M_{\theta,1} \theta_A \theta_B.\end{aligned}\quad (50)$$

The matrix elements appearing here depend on the original state (x -parallel, etc., found earlier in II B). The equations of motion [23] are especially simple in matrix notation,

$$\dot{\psi}_\phi = 2\frac{\gamma}{\mu} M_\theta \psi_\theta, \quad \dot{\psi}_\theta = -2\frac{\gamma}{\mu} M_\phi \psi_\phi. \quad (51)$$

When combined they give separated eigenvalue problems,

$$\begin{aligned}\ddot{\psi}_\phi &= -\omega^2 \psi_\phi = -\left(2\frac{\gamma}{\mu}\right)^2 M_\theta M_\phi \psi_\phi, \\ \ddot{\psi}_\theta &= -\omega^2 \psi_\theta = -\left(2\frac{\gamma}{\mu}\right)^2 M_\phi M_\theta \psi_\theta.\end{aligned}\quad (52)$$

These are identical eigenvalue problems, due to the symmetric structure of the matrices, and they determine the eigenfrequencies. We already know that the eigenvectors for both matrices are $\psi^\pm = \frac{1}{\sqrt{2}}(1, \pm 1)$ and hence also for their products. That means the ϕ and θ oscillations have the same frequencies, determined by the eigenvalues σ of the M_θ and M_ϕ matrices,

$$\omega^\pm = 2\frac{\gamma}{\mu} \sqrt{\sigma_\theta^\pm \sigma_\phi^\pm}. \quad (53)$$

This necessarily requires that the θ and ϕ components are either both in the ψ^+ eigenstate or both in the ψ^- eigenstate. It shows how the energy eigenvalues from H_{AB} connect to the dynamics, and that the state is unstable if the product $\sigma_\theta \sigma_\phi$ becomes negative. When ω^+ goes to zero, the instability first appears at $qa = 0$ (symmetrized sublattices), but if ω^- goes to zero, the instability is at $qa = \pi$ (antisymmetrized sublattices).

A. Using the full chain Hamiltonian, nearest neighbor model

The full N -site chain linearized dynamics comes from Hamiltonian (2) approximated quadratically in deviations (θ_n, ϕ_n) around one of the stable states. Thus

putting $\phi_n \rightarrow \bar{\phi}_n + \phi_n$, the Hamiltonian

$$H = \sum_{n=1}^N \left[D \left\{ \sin \theta_n \sin \theta_{n+1} + \cos \theta_n \cos \theta_{n+1} \times \right. \right. \\ \left. \left. [-2 \cos(\bar{\phi}_n + \phi_n) \cos(\bar{\phi}_{n+1} + \phi_{n+1}) \right. \right. \\ \left. \left. + \sin(\bar{\phi}_n + \phi_n) \sin(\bar{\phi}_{n+1} + \phi_{n+1}) \right] \right\} \\ - K_1 \cos^2 \theta_n \sin^2(\bar{\phi}_n + \phi_n) + K_3 \sin^2 \theta_n \left. \right] \quad (54)$$

is to be expanded. The deviations are vectors of the in-plane and out-of-plane deviation angles,

$$\psi_\phi^\dagger = (\phi_1, \phi_2, \phi_3, \dots, \phi_N), \quad \psi_\theta^\dagger = (\theta_1, \theta_2, \theta_3, \dots, \theta_N). \quad (55)$$

The system Hamiltonian has static state energy \bar{H} plus quadratic contributions of deviations involving 0th and 1st neighbors, $H \approx \bar{H} + \psi_\phi^\dagger M_\phi \psi_\phi + \psi_\theta^\dagger M_\theta \psi_\theta$, or

$$H \approx \bar{H} + \sum_n \left[M_{\phi,0} \phi_n^2 + 2M_{\phi,1} \phi_n \phi_{n+1} \right. \\ \left. + M_{\theta,0} \theta_n^2 + 2M_{\theta,1} \theta_n \theta_{n+1} \right] \quad (56)$$

where the matrices are of tridiagonal form,

$$M_\phi = \begin{pmatrix} M_{\phi,0} & M_{\phi,1} & 0 & 0 & \dots \\ M_{\phi,1} & M_{\phi,0} & M_{\phi,1} & 0 & \dots \\ 0 & M_{\phi,1} & M_{\phi,0} & M_{\phi,1} & \dots \\ 0 & 0 & M_{\phi,1} & M_{\phi,0} & \dots \\ 0 & 0 & 0 & M_{\phi,1} & \dots \\ \dots & \dots & \dots & \dots & \dots \end{pmatrix}. \quad (57)$$

The diagonal ($M_{\phi,0}$) and nearest neighbor ($M_{\phi,1}$) matrix elements depend on the unperturbed state, see following subsections. The linearized equations of motion from (56) are

$$\frac{\mu}{\gamma} \dot{\phi}_n = + \frac{\partial H}{\partial \theta_n} = + 2M_{\theta,0} \theta_n + 2M_{\theta,1} (\theta_{n-1} + \theta_{n+1}), \\ \frac{\mu}{\gamma} \dot{\theta}_n = - \frac{\partial H}{\partial \phi_n} = - 2M_{\phi,0} \phi_n - 2M_{\phi,1} (\phi_{n-1} + \phi_{n+1}). \quad (58)$$

These are very compact in matrix notation,

$$\dot{\psi}_\phi = 2 \frac{\gamma}{\mu} M_\theta \psi_\theta, \quad \dot{\psi}_\theta = - 2 \frac{\gamma}{\mu} M_\phi \psi_\phi. \quad (59)$$

Each matrix operator has eigenvalues, $\lambda_\phi^{(m)}$, $\lambda_\theta^{(m)}$, with

$$M_\phi \psi_\phi^{(m)} = \lambda_\phi^{(m)} \psi_\phi^{(m)}, \quad M_\theta \psi_\theta^{(m)} = \lambda_\theta^{(m)} \psi_\theta^{(m)}, \quad (60)$$

where (m) labels a simultaneous eigenvector of both M_ϕ and M_θ . Then the mode eigenfrequencies are

$$\omega^{(m)} = 2 \frac{\gamma}{\mu} \sqrt{\lambda_\phi^{(m)} \lambda_\theta^{(m)}}. \quad (61)$$

Due to the symmetric form of the matrices for this 1D problem, the dynamic mode eigenvalues $\omega^{(m)}$ then are determined from the general energy eigenvalues for deviations around the stable states.

B. The eigenvalues for traveling wave solutions

Consider traveling wave solutions and the eigenvalues of the M -matrices. With allowed wave vectors on a chain, $q = 2\pi m/Na$, and a parameter $r \equiv e^{iqa}$, an assumed solution is

$$\phi_n = \phi r^n, \quad \theta_n = \theta r^n, \quad (62)$$

where ϕ and θ without subscripts are wave amplitudes at some origin $n = 0$. From (58), one row of the M_ϕ matrix acting on ψ_ϕ in the eigenvalue problem (60) is

$$\lambda_\phi \phi r^n = [M_{\phi,0} + M_{\phi,1}(r^{-1} + r^{+1})] \phi r^n. \quad (63)$$

The eigenvalues of M_ϕ and M_θ easily result,

$$\lambda_\phi(q) = M_{\phi,0} + 2M_{\phi,1} \cos qa, \\ \lambda_\theta(q) = M_{\theta,0} + 2M_{\theta,1} \cos qa. \quad (64)$$

These eigenvalues then can be applied in expression (61) and the dynamic mode frequencies are determined in the nearest neighbor model, for each of the stable states, provided that M_ϕ and M_θ have been determined. The wave vector q plays the role of the mode index m .

1. Modes around x -parallel states

For the x -parallel state with $\bar{\phi}_n = 0$, the expansion of (54) leads to $\bar{H} = -2ND$ and matrix elements,

$$M_{\phi,0} = 2D - K_1, \quad M_{\phi,1} = \frac{1}{2}D, \\ M_{\theta,0} = 2D + K_3, \quad M_{\theta,1} = \frac{1}{2}D. \quad (65)$$

Then the q -dependent eigenvalues are

$$\lambda_\phi(q) = D(2 + \cos qa) - K_1, \\ \lambda_\theta(q) = D(2 + \cos qa) + K_3. \quad (66)$$

Using (61), the resulting mode frequencies are

$$\frac{\omega(q)}{4\delta_1} = \sqrt{(1 + \frac{1}{2} \cos qa - \frac{K_1}{2D})(1 + \frac{1}{2} \cos qa + \frac{K_3}{2D})}, \quad (67)$$

which are the same as the earlier result (34) obtained from undamped dynamics.

2. Modes around y -parallel states

In a y -parallel state with $\bar{\phi}_n = \frac{\pi}{2}$, the expansion of the Hamiltonian (54) leads to $\bar{H} = N(D - K_1)$, while the matrix elements are

$$M_{\phi,0} = -D + K_1, \quad M_{\phi,1} = -D, \\ M_{\theta,0} = -D + K_1 + K_3, \quad M_{\theta,1} = \frac{1}{2}D. \quad (68)$$

That means the q -dependent eigenvalues are

$$\begin{aligned}\lambda_\phi(q) &= -D(1 + 2 \cos qa) + K_1, \\ \lambda_\theta(q) &= D(-1 + \cos qa) + K_1 + K_3.\end{aligned}\quad (69)$$

The y -parallel states require $K_1 > 3D$ for stability, so both of these eigenvalues are positive for any allowed q . Applying (61), the dynamic mode frequencies are

$$\frac{\omega(q)}{2\delta_1} = \sqrt{(-1 - 2 \cos qa + \frac{K_1}{D}) (-1 + \cos qa + \frac{K_{13}}{D})}.\quad (70)$$

This agrees with the earlier result (37), although here it has been written such that both factors inside the square root are positive when y -parallel is stable.

3. Modes around y -alternating states

For a y -alternating state with $\bar{\phi}_n = (-1)^n \frac{\pi}{2}$, the expansion of the Hamiltonian (54) gives $\bar{H} = -N(D + K_1)$, and the matrix elements are

$$\begin{aligned}M_{\phi,0} &= D + K_1, & M_{\phi,1} &= D, \\ M_{\theta,0} &= D + K_1 + K_3, & M_{\theta,1} &= \frac{1}{2}D.\end{aligned}\quad (71)$$

The resulting q -dependent eigenvalues are

$$\begin{aligned}\lambda_\phi(q) &= D(1 + 2 \cos qa) + K_1, \\ \lambda_\theta(q) &= D(1 + \cos qa) + K_1 + K_3.\end{aligned}\quad (72)$$

Both of these eigenvalues are positive for any q as long as $K_1 > D$, which is the previously found stability requirement. The dynamic mode frequencies become

$$\frac{\omega(q)}{2\delta_1} = \sqrt{(1 + 2 \cos qa + \frac{K_1}{D}) (1 + \cos qa + \frac{K_{13}}{D})}.\quad (73)$$

That agrees with the earlier result (44) for the g -modes of a y -alternating state.

V. INCLUDING LONG-RANGE DIPOLE INTERACTIONS

Long-range dipole interactions (LRD) can be included easily in the energy analysis. The dipolar interaction strength in (2) is D at the nearest neighbor distance a . This energy factor behaves as $1/r^3$. So for 2nd nearest neighbors, the strength will be $D/2^3$; for 3rd nearest neighbors it is $D/3^3$, and so on. Along a 1D chain, the sum of all neighbors' energies to any distance can be constructed.

Only the first neighbor dipole terms were used in Eq. (54), as indicated in the subscripts $n + 1$. For the contribution of pairs of k^{th} neighbors (at separation distance

ka), the dipolar part of the Hamiltonian is

$$H_k = \frac{D}{k^3} \sum_{n=1}^N \left\{ \sin \theta_n \sin \theta_{n+k} + \cos \theta_n \cos \theta_{n+k} \times \right. \\ \left. [-2 \cos(\bar{\phi}_n + \phi_n) \cos(\bar{\phi}_{n+k} + \phi_{n+k}) + \sin(\bar{\phi}_n + \phi_n) \sin(\bar{\phi}_{n+k} + \phi_{n+k})] \right\}.\quad (74)$$

For k^{th} neighbors, the zeroth, linear and quadratic terms in angular deviations are obtained by expanding (74), which is most tractable when done separately for each meta-state.

A. LRD in x -parallel states

For x -parallel states ($\bar{\phi}_n = 0$), expansion of (74) up to quadratic deviation terms for $k \geq 1$ gives

$$H_k \approx \frac{D}{k^3} \sum_{n=1}^N (-2 + 2\phi_n^2 + \phi_n \phi_{n+k} + 2\theta_n^2 + \theta_n \theta_{n+k}).\quad (75)$$

The first term modifies the unperturbed x -parallel state energy by an amount $\bar{H}_k = -\frac{2}{k^3}ND$, and the others are quadratic interactions. This implies shifts to the diagonal matrix elements [denoted $\Delta M_{\phi,0}^{(k)}$] and new elements ($M_{\phi,k}$) for k^{th} neighbor couplings,

$$\begin{aligned}\Delta M_{\phi,0}^{(k)} &= \frac{2D}{k^3}, & M_{\phi,k} &= \frac{D}{2k^3}, \\ \Delta M_{\theta,0}^{(k)} &= \frac{2D}{k^3}, & M_{\theta,k} &= \frac{D}{2k^3}.\end{aligned}\quad (76)$$

For example, keeping only 0th, 1st and 2nd nearest neighbors, a row of the eigenvalue problem, $M_\phi \psi_\phi = \lambda_\phi \psi_\phi$, is

$$\begin{aligned}M_{\phi,0}\phi_n + M_{\phi,1}(\phi_{n-1} + \phi_{n+1}) \\ + M_{\phi,2}(\phi_{n-2} + \phi_{n+2}) = \lambda_\phi \phi_n,\end{aligned}\quad (77)$$

With the x -parallel matrix elements, this becomes

$$\begin{aligned}(2D + \frac{1}{4}D - K_1) \phi_n + \frac{1}{2}D(\phi_{n-1} + \phi_{n+1}) \\ + \frac{1}{16}D(\phi_{n-2} + \phi_{n+2}) = \lambda_\phi \phi_n.\end{aligned}\quad (78)$$

Using the traveling wave solution (62) with $\phi_n \propto r^n$, the eigenvalue by including up to 2nd neighbors is

$$\lambda_\phi = -K_1 + D(2 + \cos qa) + \frac{1}{8}D(2 + \cos 2qa).\quad (79)$$

The first two terms come from the nearest neighbor model, see (66). The last term shows the effect of 2nd neighbor interactions. It contains a shift by $\frac{1}{4}D$, as well as a dependence on the doubled wave vector.

Third neighbors will have factors of $\frac{D}{3^3}$ and $\cos 3qa$, and so on for farther neighbors. Assuming a chain of

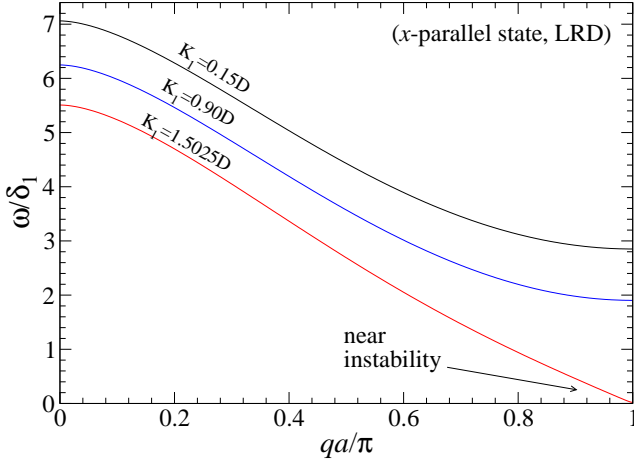


FIG. 6: Mode frequencies for x -parallel states, including all long range dipole interactions, with $K_3 = 0$. The modes produce instability (ω acquires an imaginary part) near $qa = \pi$ as $K_1 \rightarrow 1.502571 D$. The states have a greater range of stability than in the nearest neighbor model.

infinite length, the eigenvalue is a sum over increasingly distant neighbor interactions,

$$\lambda_\phi = \sum_{k=1}^{\infty} \left[\Delta M_{\phi,0}^{(k)} + 2M_{\phi,k} \cos kqa \right]. \quad (80)$$

For x -parallel states this gives

$$\begin{aligned} \lambda_\phi(q) &= -K_1 + D \sum_{k=1}^{\infty} \frac{1}{k^3} (2 + \cos kqa) \\ &= -K_1 + D [2\zeta(3) + \text{Cl}_3(qa)]. \end{aligned} \quad (81)$$

This is written using the Riemann zeta function, whose needed value is $\zeta(3) \approx 1.20205$, combined with a Clausen function of order 3.

For the out-of-plane eigenvalue, the same procedure applies, but with $-K_1$ replaced by $+K_3$ (see Eq. 65),

$$\begin{aligned} \lambda_\theta(q) &= K_3 + D \sum_{k=1}^{\infty} \frac{1}{k^3} (2 + \cos kqa) \\ &= K_3 + D [2\zeta(3) + \text{Cl}_3(qa)]. \end{aligned} \quad (82)$$

According to (61), they give the eigenfrequencies,

$$\frac{\omega(q)}{4\delta_1} = \sqrt{\left[-\frac{K_1}{2D} + \zeta(3) + \frac{1}{2}\text{Cl}_3(qa) \right] \left[\frac{K_3}{2D} + \zeta(3) + \frac{1}{2}\text{Cl}_3(qa) \right]}. \quad (83)$$

This is a simple modification of the frequencies in the nearest neighbor model, Eq. (67), but where $\text{Cl}_3(qa)$ replaces $\cos qa$, and $\zeta(3)$ has replaced a factor of 1. Some typical dispersion relations are shown in Fig. 6.

Stability of the x -parallel state requires both eigenvalues to remain positive for any q . The most negative value of the Clausen function occurs at $qa = \pi$, where $2\zeta(3) + \text{Cl}_3(\pi) = 1.502571\dots$ That means λ_θ is always

positive, but λ_ϕ remains positive and the state is stable only as long as

$$K_1/D < 1.502571. \quad (84)$$

That is a 50% increase compared to the nearest neighbor model.

B. LRD in y -parallel states

The same procedure can be applied to longer range dipolar interactions for y -parallel states, such as the one with all $\bar{\phi}_n = \frac{\pi}{2}$. Consider neighbors at separation distance ka . From expansion of (74), the dipolar energy of k^{th} -neighbor pairs to quadratic order in deviations is

$$H_k \approx \frac{D}{k^3} \sum_{n=1}^N (1 - \phi_n^2 - 2\phi_n\phi_{n+k} - \theta_n^2 + \theta_n\theta_{n+k}). \quad (85)$$

The first term modifies the unperturbed y -parallel state energy by the amount $\bar{H}_k = \frac{1}{k^3}ND$. The other parts determine the changes to diagonal matrix elements, and new elements for k^{th} neighbors,

$$\begin{aligned} \Delta M_{\phi,0}^{(k)} &= -\frac{D}{k^3}, & M_{\phi,k} &= -\frac{D}{k^3}, \\ \Delta M_{\theta,0}^{(k)} &= -\frac{D}{k^3}, & M_{\theta,k} &= +\frac{D}{2k^3}. \end{aligned} \quad (86)$$

As a specific example, when keeping up to 2nd neighbor dipole interactions, the in-plane eigenequation becomes

$$\begin{aligned} (-D + K_1 - \frac{1}{8}D) \phi_n - D(\phi_{n-1} + \phi_{n+1}) \\ - \frac{1}{8}D(\phi_{n-2} + \phi_{n+2}) = \lambda_\phi \phi_n. \end{aligned} \quad (87)$$

The 3rd neighbors will be similar but with a factor of $\frac{1}{27}$, and so on, so that the result including arbitrarily distant dipole terms is

$$\begin{aligned} \lambda_\phi(q) &= K_1 - D \sum_{k=1}^{\infty} \frac{1}{k^3} (1 + 2 \cos kqa) \\ &= K_1 - D [\zeta(3) + 2\text{Cl}_3(qa)]. \end{aligned} \quad (88)$$

The same procedure applies to the out-of-plane system, but with K_1 replaced by K_{13} and using $M_{\theta,1} = \frac{1}{2}D$ instead of $M_{\phi,1} = -D$, see Eq. (68). The eigenvalues are

$$\begin{aligned} \lambda_\theta(q) &= K_1 + K_3 + D \sum_{k=1}^{\infty} \frac{1}{k^3} (-1 + \cos kqa) \\ &= K_{13} + D [-\zeta(3) + \text{Cl}_3(qa)]. \end{aligned} \quad (89)$$

This gives the mode dispersion relation,

$$\frac{\omega(q)}{2\delta_1} = \sqrt{\left[\frac{K_1}{D} - \zeta(3) - 2\text{Cl}_3(qa) \right] \left[\frac{K_{13}}{D} - \zeta(3) + \text{Cl}_3(qa) \right]}. \quad (90)$$

The dispersion relation is shown in Fig. 7 for a few values of anisotropy. For stability, both factors within the

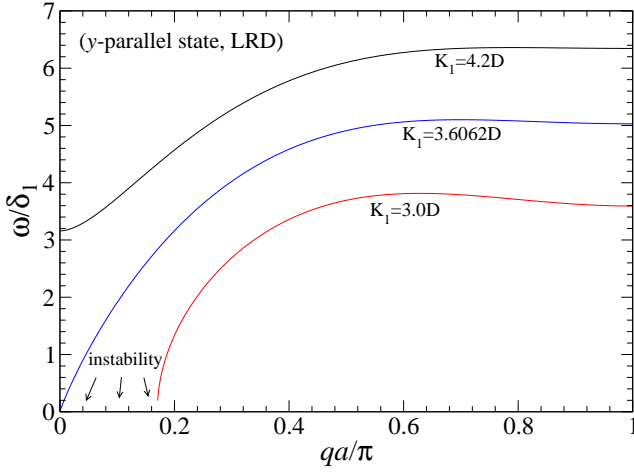


FIG. 7: Mode frequencies for y -parallel states, including all long range dipole interactions, with $K_3 = 0$. The modes produce instability (ω has an imaginary part) near $qa = 0$ as $K_1 \rightarrow 3.60617 D$ from above. For example, y -parallel is unstable for $K_1/D = 3$, as indicated by the presence of an imaginary frequency.

square root must be positive. When $q = 0$, one has $\text{Cl}_3(0) = \zeta(3)$, which shows that stability requires

$$K_1/D > 3\zeta(3) \approx 3.606, \quad (91)$$

which is a 20% increase over the stability limit on K_1 in the nearest neighbor model.

C. LRD in y -alternating states

The analysis of y -alternating states, such as the one with $\bar{\phi}_n = (-1)^n \frac{\pi}{2}$, is different from that for the parallel states, because 2nd, 4th, etc. neighbor spins are aligned, while 1st, 3rd, etc. neighbor spins are antialigned.

In a y -alternating state, the in-plane factors in the dipolar energy H_k [Eq. (74)] for k^{th} neighbor pairs are

$$\begin{aligned} \sin(\bar{\phi}_n + \phi_n) \sin(\bar{\phi}_{n+k} + \phi_{n+k}) &\approx (-1)^k \left(1 - \frac{1}{2}\phi_n^2 - \frac{1}{2}\phi_{n+k}^2\right), \\ -2 \cos(\bar{\phi}_n + \phi_n) \cos(\bar{\phi}_{n+k} + \phi_{n+k}) &\approx (-1)^k (-2\phi_n \phi_{n+k}). \end{aligned} \quad (92)$$

The overall sign on these factors alternates with the separation, because a pair of dipoles perpendicular to the chain will lower their energy by being antiparallel. Then the dipolar energy (74) is approximated as

$$\begin{aligned} H_k &\approx \frac{D}{k^3} \sum_{n=1}^N \left[\theta_n \theta_{n+k} + \left(1 - \frac{1}{2}\theta_n^2 - \frac{1}{2}\theta_{n+k}^2\right) \right. \\ &\quad \left. \times (-1)^k \left(1 - \frac{1}{2}\phi_n^2 - \frac{1}{2}\phi_{n+k}^2 - 2\phi_n \phi_{n+k}\right) \right] \\ &\approx \frac{D}{k^3} \sum_{n=1}^N \left[\theta_n \theta_{n+k} + (-1)^k \left(1 - \phi_n^2 - 2\phi_n \phi_{n+k} - \theta_n^2\right) \right]. \end{aligned} \quad (93)$$

From that, the contribution to the energy of the y -alternating state is $\bar{H}_k = \frac{(-1)^k}{k^3} N D$. The shifts in diagonal matrix elements and the elements for k^{th} neighbors are

$$\begin{aligned} \Delta M_{\phi,0}^{(k)} &= -\frac{(-1)^k D}{k^3}, & M_{\phi,k} &= -\frac{(-1)^k D}{k^3}, \\ \Delta M_{\theta,0}^{(k)} &= -\frac{(-1)^k D}{k^3}, & M_{\theta,k} &= \frac{D}{2k^3}. \end{aligned} \quad (94)$$

Then the sum in (80) gives the in-plane eigenvalues,

$$\lambda_\phi(q) = K_1 - D \sum_{k=1}^{\infty} \frac{(-1)^k}{k^3} (1 + 2 \cos kqa) \quad (95)$$

This alternating series is obtained from a Clausen function, at a shifted argument, *viz.*

$$\begin{aligned} \text{Cl}_3(qa + \pi) &= \sum_{k=1}^{\infty} \frac{1}{k^3} \cos[k(qa + \pi)] \\ &= \sum_{k=1}^{\infty} \frac{1}{k^3} \cos k\pi \cos kqa = \sum_{k=1}^{\infty} \frac{(-1)^k}{k^3} \cos kqa. \end{aligned} \quad (96)$$

With the particular value, $\text{Cl}_3(\pi) = \sum_{n=1}^{\infty} \frac{(-1)^n}{n^3} \approx -0.90154\dots$, the eigenvalues are

$$\lambda_\phi(q) = K_1 - D [\text{Cl}_3(\pi) + 2\text{Cl}_3(qa + \pi)]. \quad (97)$$

For the out-of-plane eigenvalues, a sum like that in (80) with the corresponding matrix elements gives

$$\begin{aligned} \lambda_\theta(q) &= K_{13} - D \sum_{k=1}^{\infty} \frac{1}{k^3} ((-1)^k + \cos kqa) \\ &= K_{13} + D [-\text{Cl}_3(\pi) + \text{Cl}_3(qa)]. \end{aligned} \quad (98)$$

Then the mode dispersion relation is

$$\begin{aligned} \frac{\omega(q)}{2\delta_1} &= \left[\frac{K_1}{D} - \text{Cl}_3(\pi) - 2\text{Cl}_3(qa + \pi) \right]^{1/2} \\ &\quad \times \left[\frac{K_{13}}{D} - \text{Cl}_3(\pi) + \text{Cl}_3(qa) \right]^{1/2}. \end{aligned} \quad (99)$$

Note how the factor $\text{Cl}_3(\pi)$ for the y -alternating states replaces $\text{Cl}_3(0) = \zeta(3)$ that appears for y -parallel states, and there is the shifted argument of the Clausen function from the in-plane eigenvalue. Example dispersion relations are shown in Fig. 8. Regarding stability, λ_θ is always positive, so instability occurs when λ_ϕ becomes negative. Thus, the requirement on K_1 for stable y -alternating states is

$$\frac{K_1}{D} > [\text{Cl}_3(\pi) + 2\text{Cl}_3(qa + \pi)]|_{qa \rightarrow \pi} \approx 1.502571\dots \quad (100)$$

This is the same anisotropy strength above which the x -parallel state goes unstable.

D. State energies with all dipole interactions

It is important also to get the per-site energy, $u = H/N$, including all long range dipole interactions. That

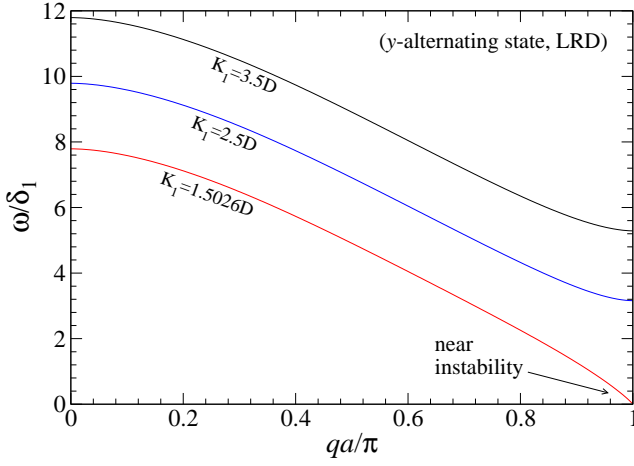


FIG. 8: Mode frequencies for y -alternating states, including all long range dipole interactions, with $K_3 = 0$. The modes produce instability near $qa = \pi$ as $K_1 \rightarrow 1.502571 D$ from above.

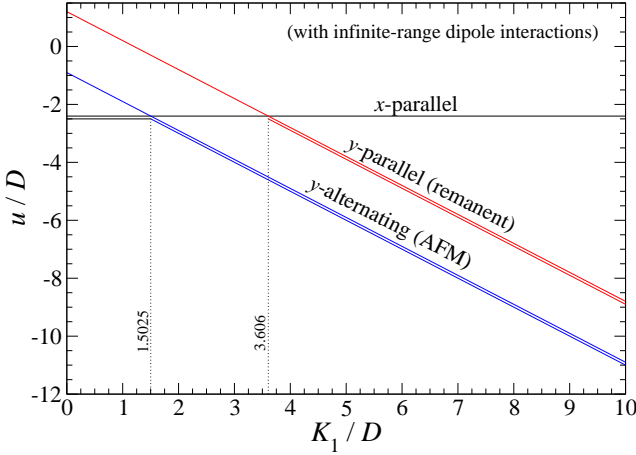


FIG. 9: The static per-site energies of the three types of states, when all long-range dipole interactions are included. The x -parallel states are now stable only for $K_1 < 1.50257 D$, y -alternating for $K_1 > 1.50257 D$, and y -parallel for $K_1 > 3.606 D$. Double (single) lines indicate local stability (instability) against weak perturbations.

involves combining the \bar{H}_k contributions and anisotropy contributions. For x -parallel states, the sum is,

$$u = \sum_{k=1}^{\infty} \frac{-2D}{k^3} = -2D\zeta(3) \approx -2.404 D. \quad (101)$$

That is $-0.404 D$ lower than that from the nearest neighbor model. Along with the wider range of K_1 that insures stability, this shows that long range dipole interactions help to stabilize the x -parallel states.

For y -parallel states, the per-site energy is

$$\begin{aligned} u &= -K_1 + \sum_{k=1}^{\infty} \frac{D}{k^3} \\ &= -K_1 + D\zeta(3) \approx -K_1 + 1.202 D. \end{aligned} \quad (102)$$

That is $0.202 D$ higher than found for the nearest neighbor model. Viewed together with the modified stability requirement, this indicates that long range dipole interactions slightly reduce the stability of y -parallel states.

For y -alternating states, the energy per site becomes

$$\begin{aligned} u &= -K_1 + \sum_{k=1}^{\infty} \frac{(-1)^k D}{k^3} \\ &= -K_1 + DCl_3(\pi) \approx -K_1 - 0.9015 D. \end{aligned} \quad (103)$$

That is $0.0985 D$ higher than found in the nearest neighbor model, because 2nd neighbor dipoles are antialigned and have high dipolar energy.

The energies of all three states are summarized graphically in Fig. 9. This analysis indicates that y -parallel and y -alternating states are both locally stable in the regime where $K_1/D > 3\zeta(3)$, even though y -alternating states have lower energy.

VI. DISCUSSION & CONCLUSIONS

An array of elongated magnetic islands arranged as in Fig. 1 has been shown to have three uniform states, whose linear stability depends on the uniaxial anisotropy strength K_1 relative to the nearest neighbor dipolar interaction strength D . The conclusions are reached both by looking at the behavior of the states' energy-related eigenvalues λ_ϕ and λ_θ , and the related frequencies of the linearized oscillations about the states.

Including infinite range dipole interactions, the states' linear stability regimes, shown in Fig. 9 with double lines, are summarized as follows. At very weak anisotropy ($K_1 < 1.50257 D$), the x -parallel states will be the only stable states, where the dipoles minimize their dipolar energy with little cost in anisotropy energy. For an intermediate range of anisotropy ($1.50257 D < K_1 < 3.606 D$), the AFM-ordered y -alternating states have the lowest energy and become the only stable states. Both the dipolar and anisotropy energies are minimized. For strong anisotropy ($3.606 D < K_1$), the y -alternating states still have the lowest energy and are stable. The remanent FM-ordered y -parallel states are locally stable against small perturbations (they have only positive λ_ϕ and λ_θ eigenvalues), although they are higher in energy than the y -alternating states by $2.103 D$. They would be metastable with respect to strong perturbations. In the y -parallel remanent states, the anisotropy energy is minimized and dominates greatly over the non-optimal dipolar energy.

The remanent states could be produced experimentally by application of a magnetic field transverse to the chain,

which is slowly turned off. The y -alternating states could be obtained from a remanent state either by application of a field along the chain (x) direction, which is then reduced to zero, or, by a field opposite to the original direction of magnetization. Other switching between states might be implemented with the help of AC and rotating demagnetization protocols as used in square and rectangular lattice artificial magnetic ice [24–26] to reach its various states.

This type of system might be the basis for new detectors or devices, and allows for various ways to con-

trol the design. Although a static island array will have fixed values of K_1 and D , one can imagine these might be modulated, for example, by applying pressure [19] to an elastic substrate or other modified new materials. If the system is designed near one of the critical anisotropy points ($K_1 \approx 1.50257 D$ or $K_1 \approx 3.606 D$), it might be possible to induce a strain in the medium that shifts the stability point between two of the states. Alternatively, application of magnetic fields may be sufficient to control switching between the y -alternating and y -parallel states. These effects invite further investigation.

-
- [1] Nguyen V *et al.* 2017 *Phys. Rev. B* **96** 014402
- [2] Östman E *et al.* 2018 *J. Phys.: Condens. Matter* **30** 365301
- [3] Cisternas J *et al.* 2021 *Phys. Rev. B* **103** 134443
- [4] Skjærvø S H, Marrows C H, Stamps R L and Heyderman L J, 2020 *Nat. Rev. Phys.* **2** 13
- [5] Ising E 1925 *Z. Physik* **31** 253
- [6] Onsager L 1944 *Phys. Rev.* **65** 117
- [7] Wang R F, Nisoli C, Freitas R S, Li J, McConville W, Cooley B J, Lund M S, Samarth N, Leighton C, Crespi V H and Schiffer P 2006 *Nature* **439** 303
- [8] Nisoli C, Moessner R and Schiffer P 2013 *Rev. Mod. Phys.* **85** 1473
- [9] Morgan J P, Stein A, Langridge S, and Marrows C, 2011 *Nature Phys.* **7** 75
- [10] Iacocca E, Gliga S, Stamps R L, and Heinonen O 2016 *Phys. Rev. B* **93** 134420
- [11] Lasnier T D and Wysin G M 2020 *Phys. Rev. B* **101** 224428
- [12] Gliga S, Kákay A, Hertel R, and Heinonen O G 2013 *Phys. Rev. Lett.* **110** 117205 .
- [13] Jungfleisch M B *et al.* 2016 *Phys. Rev. B* **93** 100401(R)
- [14] Arroo D M, Gartside J C, and Branford W R 2019 *Phys. Rev. B* **100** 214425
- [15] Arora N and Das P 2021 *AIP Advances* **11** 035030
- [16] Heisenberg W 1928 *Z. Phys.* **49** 619
- [17] Jiles David *Introduction to Magnetism and Magnetic Materials* (London: Chapman and Hall) Ch 11
- [18] Wysin G M, Moura-Melo W A, Mól L A S and Pereira A R 2012 *J. Phys.: Condens. Matter* **24** 296001
- [19] Edberg R 2021 Spin ice under uniaxial pressure and magnetic frustration in garnets *PhD dissertation* KTH Royal Institute of Technology, Nordforsk, (<http://urn.kb.se/resolve?urn=urn:nbn:se:kth:diva-293527>)
- [20] Wysin G M, Moura-Melo W A, Mól L A S and Pereira A R 2013 *New J. Phys.* **15** 045029
- [21] Wysin G M, Pereira A R, Moura-Melo W A and de Araujo C I L 2015 *J. Phys.: Condens. Matter* **27** 076004
- [22] Shevchenko Y, Makarov A and Nefedev K 2017 *Phys. Lett. A* **381(5)** 428-434
- [23] Wysin G M 2015 *Magnetic Excitations & Geometric Confinement: Theory and Simulations* (London: IOP Expanding Physics ebook) Ch 2
- [24] Ke X *et al.* 2008 *Phys. Rev. Lett.* **101** 037205
- [25] Nisoli C *et al.* 2010 *Phys. Rev. Lett.* **105** 047205
- [26] Ribeiro I R B *et al.* 2017 *Scientific Reports* **7**, 13982